Application of a 3D Lagrangian model to explain the decline of a *Dinophysis acuminata* bloom in the Bay of Biscay

Velo-Suárez, L.[1*], Reguera, B.[1], González-Gil, S.[2], Lunven, M.[3], Lazure, P.[3], Nézan, E.[4], and Gentien, P.[3]

[1] *Instituto Español de Oceanografía, Centro Oceanográfico de Vigo, Aptdo. 1552, E-36200 Vigo, Spain*

[2] *Instituto Español de Oceanografía, Centro Oceanográfico de Madrid, Orense 58, 7ª planta, E- 28020 Madrid, Spain*

[3] *IFREMER, Centre de Brest. DYNECO. Pointe du Diable BP70, E-29280 Plouzane, France*

[4] *IFREMER, 13, rue de Kérose, Le Roudouic E-29187 Concarneau Cedex, France*

* Corresponding author:
Lourdes Velo-Suárez
Instituto Español de Oceanografía
Centro Oceanográfico de Vigo
Aptdo. 1552, E-36280 Vigo, Spain
Tel: 34-986-492111
Fax: 34-986-498626
e-mail: lourdesvelo@gmail.es

Abstract

During July 2006, a cruise was carried out in the Northern Bay of Biscay (off Brittany, France) to study meso-and microscale patterns of phytoplankton distribution. Special attention was focused on the fine scale vertical distribution of *Dinophysis* spp. and its physiological status. Moderate concentrations (10^2-10^3 cells L^{-1}) of *Dinophysis acuminata* were constrained to specific depths (upper layers of the pycnocline) at stations with lower surface salinity (34.5) and steep temperature gradients (18-13.5ºC between 04 and 07 m depth) within the Loire and Vilaine river plumes. On board observations showed a *D. acuminata* population at the maxima with 89% of viable (FDA-treated) cells and moderate growth (up to 0.23 d^{-1}) in cell isolates that showed a positive growth response to DOM (M.W.>1 kD) from the same area concentrated by ultrafiltration. Despite the good physiological conditions of the cells, the population of *D. acuminata* declined rapidly to undetectable levels during the second leg of the cruise. For the first time a 3D Lagrangian Particle Tracking Model was used to explore the effect of physical dispersion in the decline of a *Dinophysis* bloom in the Loire and Vilaine river plumes (Bay of Biscay) during the exceptionally hot summer of 2006.

Keywords: Lagrangian individual particle tracking models, harmful algal blooms, *Dinophysis acuminata*, physical-biological interactions, Bay of Biscay.

1. Introduction

Diarrhetic shellfish poisoning (DSP) is a gastrointestinal disease resulting from ingestion of shellfish contaminated with OA-related lipophilic dinoflagellate toxins. These toxins threaten public health and shellfish industries due to its worldwide occurrence, high morbidity rate and the long duration of shellfish toxicity outbreaks even at very minute ($< 10^2$ cells L^{-1}) cell concentrations (Yasumoto et al., 1985).

The French Phytoplankton Monitoring Network (REPHY) was created by the IFREMER (Institut Français de Recherche pour l'Exploitation de la Mer) in 1984 to detect the seasonal occurrence of potentially toxic dinoflagellates, with emphasis on *Dinophysis* species. Since then, seasonal blooms of *D. acuminata* associated with DSP outbreaks have been nearly annual features in different regions of the Bay of Biscay (France) (Delmas et al., 1992).

Unveiling the nutritional sources for *Dinophysis* spp. has been a challenge for decades. Nevertheless, recent work has shown *D. acuminata* to be a mixotroph that grows well when feeding on the photosynthetic ciliate *Mesodinium rubrum* (= *Myrionecta rubra*) (Park et al., 2006). Recent culture results have suggested that *D. acuminata* is an obligate mixotroph that requires light, nutrients and live ciliate prey for long-term survival (Kim et al., 2008; Riisgaard and Hansen, 2009). Evidences of *D. acuminata* blooms promoted by elevated inorganic nutrient concentrations have not been found (Delmas et al., 1992). In contrast, a co-occurrence of *Dinophysis* maxima and that of organic matter aggregates has been reported by several authors (Gentien et al., 1995; Lunven et al., 2003).

Different mechanisms have been suggested for the control of the initiation and development of dinoflagellate blooms. Nevertheless, little is known about the factors that trigger the decline of *Dinophysis* blooms. Turbulence and currents may act to dissipate or concentrate the *D. acuminata* cells while the population numbers may change due to intrinsic features (division, mortality) and physical-biological interactions (see Velo-Suárez et al., 2009). In the coastal waters of the Northern Bay of Biscay, *D. acuminata* has been found to exhibit a very heterogeneous vertical distribution and to concentrate around water density gradients (Gentien et al., 1995; Maestrini, 1998). Different studies in the region (Lunven et al., 2005; Marcaillou et al., 2001; Lunven et al., 2005) have shown horizontal confinement of *D. acuminata* blooms in river plumes. Delmas et al. (1993) suggested a transport of *D. acuminata* populations by water inflow from offshore to coastal areas of the Northern Bay of Biscay. Following this hypothesis, Xie et al. (2007) used a 3D model under realistic forcing conditions to test the role of retention areas and their subsequent advection to the coast in promoting DSP coastal outbreaks caused by *Dinophysis* populations.

3D Lagrangian particle-tracking models (3D LPTM) and individual based models (IBM) have been used by the oceanographic community during the past two decades to explore processes that influence the transport of eggs and developing larval stages of invertebrates and fish(Gallego et al., 2007). Results from these studies have shown how this kind of models has been able to explain the transport/retention of fish larvae in some regions (Santos et al., 2007. 3D-LPTM models can provide new insights into physical-biological interactions that affect plankton dispersal, growth and survival and enhance our understanding of plankton population variability and structure (Gallego et al., 2007).

During summer 2006, a three-week multidisciplinary cruise was conducted to describe the fine-scale physical and biological structure of the water column and to study meso- and microscale patterns of phytoplankton distribution in the Northern Bay of Biscay. For this purpose, we used outputs from a realistic hydrodynamic model to force a 3D LPTM, and these simulation results are discussed together with the *D. acuminata* observations made during the survey. This work represents the first application of a 3D LPTM model to study the role of physical dispersion in the decline of a harmful dinoflagellate (*D. acuminata*) bloom located in the Loire and Vilaine river plumes, off Brittany (Bay of Biscay).

2. Material and methods

2.1. The study area

The Northern Bay of Biscay is an open bay off the West coast of France (Fig 1). Freshwater discharges from the Loire and the Vilaine Rivers into the Bay create a long-shore flow that may dominate a wide part of the continental shelf during the high-runoff season (from November to April). Propagation of the Loire and Vilaine river plumes are responsible for a marked haline stratification over the shelf that progressively weakens in summer—with the decrease in river run-off—and is the weakest at the beginning of autumn (Lazure and Jegou, 1998).

Apart from this highly variable and seasonal haline stratification, weak tidal currents in the region allow thermal stratification to be established over the entire continental shelf from spring to early autumn. Winds in the Brittany coast show an annual cycle whose

115 main characteristic is the spring (late March) shift from south-westerly to west-
116 northwesterly winds (Lazure et al., 2008).
117
118 *2.2 REPHY data*
119 Biweekly concentrations of *D. acuminata* throughout the year were obtained from
120 REPHY (IFREMER) database (http://www.ifremer.fr/envlit/surveillance/rephy.htm).
121 Phytoplankton quantitative analyses were carried out according to the Utermöhl (1931)
122 method. Samples were counted after sedimentation (4 h minimum) of 10 mL columns
123 under an inverted light microscope (IX70 Olympus) fitted with 10X, 20X and 40X
124 objectives and phase-contrast optics.
125
126 *2.3 Cruise sampling overview*
127 Studies were carried out on board R/V *Thalassa* from 06 to 22 July 2006. Sampling
128 stations from the first (06-12 July) and second (13-22 July) leg of the cruise are shown in
129 Fig 2 and Table 1. At each station, vertical plankton net (20-µm mesh; 20 m depth) hauls
130 were collected and immediately examined on board under a Nikon ECLIPSE 2000 TE-S
131 inverted microscope at 100X and 400 X magnification.
132 Measurements in the water column were carried out with the high-resolution
133 IFREMER particle size analyzer profiler (IPSAP), capable of simultaneous resolution of
134 physical and optical structures at small scale (see Gentien et al., 1995; Velo-Suárez et al.,
135 2008 for details). The IPSAP profiler includes a fluorescence sensor (Seapoint Sensors,
136 Inc., Exeter, New Hampshire, USA) attached to a SBE25 CTD probe (Sea-Bird
137 Electronics, Washington, USA) coupled to an in situ particle-size analyzer (Gentien et al.,

1995). The latter is needed as guidance for sampling, since it detects specific particle profiler, helping to distinguish between layers with abundant organic aggregates and those with dinoflagellates in the 36-64 µm fraction. The SBE25 probe allows real time data acquisition of standard parameters, such as depth, temperature, salinity, chlorophyll-like in vivo fluorescence and photosynthetically active radiation (PAR). The CTD fluorometer was calibrated with laboratory cultures of the diatom *Chaetoceros gracile* using the trichromatic method for chlorophyll determination according to Aminot and Kerouel (2004). IPSAP data were post-processed to obtain averages every 50-cm. Data presented thereafter are 50-cm averages without any overlapping.

A rosette (12 5-L Niskin bottles) attached to the IPSAP profiler was used to sample at the exact depth of the sensors. Two Niskin bottles were casted and closed at each desired depth during the upcast. After retrieval of the profiler, water samples from each bottle were immediately well mixed and then subsampled for biological and chemical analysis. From each depth, a 2-L sample was gently concentrated through a 20-µm mesh and filtered material resuspended in a volume of approximately 20 mL; 3 mL of this concentrate were poured into a sedimentation slide for in vivo observations and for a quick rough estimate of *Dinophysis* abundance. For quantitative analyses of microphytoplankton, two kinds of samples were taken: (1) unconcentrated and (2) 2-L seawater samples concentrated through 20-µm filters, that were further resuspended in a final volume of 30 mL (factor = 66.6). Samples were preserved in acidic lugol and analyzed under an inverted microscope (Nikon ECLIPSE 2000 TE-S) according to the Utermöhl (1931) method. Phytoplankton abundance was determined to species level when possible. Concentrations of smaller and more abundant species were estimated

161 from two transects counted at 400X magnification (detection limit: 40 cell L^{-1}). In the
162 case of less abundant species (including *Dinophysis* spp.), specimens from the whole
163 chamber were enumerated at a magnification of 100X after sedimentation of 3-mL
164 aliquots of the concentrated samples. In the last case, the detection limit in cell counts
165 was 5 cells L^{-1}.
166
167 *2.4* D. acuminata *in vivo observations and viability*
168 On board observations of the physiological status of *D. acuminata* from live samples
169 were performed under a Nikon ECLIPSE 2000 TE-S inverted microscope (Nikon
170 Instruments Europe B.V., The Netherlands) with Differential Interference Contrast (DIC)
171 and epifluorescence under a blue filter set (excitation 450-490 nm, emission 520 nm LP).
172 Snapshots were taken with a Nikon D70 camera coupled to the microscope at
173 magnifications of 100X and 400X. Observations included annotations on the chlorophyll
174 (red) and phaoephytin (orange) autofluorescences in *D. acuminata* and detection and
175 frequency of cells parasitized by *Amoebophrya* spp., which exhibited a characteristic
176 green autofluorescence
177 Viability assays of *D. acuminata* cells were carried out with specimens stained with
178 fluorescein diacetate (FDA; Sigma Chemicals, St Louis, MO, USA). Previous studies
179 with different vital/mortal stains (i.e SYTOX-Green, Trypan Blue, Calcein-AM) had
180 shown FDA to give the best results with natural populations of *D. acuminata* (Gónzalez-
181 Gil, Personal communication). The non-polar and non-fluorescent FDA molecules enter
182 freely into the cells and act as substrate for non-specific cell esterases. This reaction
183 results in the formation of polar and fluorescent molecules that can be retained within the

184 intact cell membrane of live cells (Coleman and Vestal, 1987). In this way, FDA stains
185 all cells with active esterases and intact cell membranes, i.e. viable cells.
186 The FDA stock solution of 5 mg mL^{-1} was dissolved in dimethyl sulfoxide (DMSO) and
187 stored at -20ºC. A portion of the previously concentrated live sample (ca. 3 mL) was
188 transferred to a sedimentation chamber and stained with 5-10 µL of the FDA working
189 solution (5 µM final concentration) and incubated in the dark for 15 min. Viable cells
190 showed green fluorescence after excitation with blue light. Red fluorescence was not
191 considered as an indication of viability since chlorophyll a in dead cells may
192 autofluoresce after cell death (Gentien, 1986). Percentages of positive and negative
193 binding were estimated after scanning of 100 cells at least of *D. acuminata* whenever
194 possible.
195
196 *2.5 Incubations with Dissolved Organic Matter (DOM) enrichment.*
197 A high flow-rate peristaltic pump on board connected by a hose to the profiler was used
198 to pump large volumes (1000 L) of seawater from the depth of the particle maximum
199 depth (18.9 m) at station 9 (see Fig 2 and Table 1 for location and date) for the DOM
200 extraction by ultrafiltration). Water was pre-filtered through 3-and 1-µm Millipore filter
201 cartridges, and then onto GF/C, GF/F (Whatmann), 0.45 µm nucleopore filters and 0.2
202 µm Opticap filter units (Millipore). DOM was concentrated by means of the Prep/scale™
203 TFF 6ft2 cartridge (Millipore) tangential ultralfiltration device (Benner et al., 1997; Guo
204 et al., 1994; Purina et al., 2004).
205 For the incubation experiments, 5 L of seawater were concentrated by reverse filtration
206 (Dodson and Thomas, 1978) through a 20-µm mesh to a final volume of about 250 mL

and maintained in the incubation chamber on board—at 15±1ºC with a 16:8 light:dark photoperiod—in glass cylinders coated with aluminium foil, except the last few centimetres near the top, to enhance accumulation of swimming dinoflagellates in the upper illuminated portion. In that way, actively swimming (healthy) cells of *D. acuminata* concentrated in a cloud near the surface as described by Maestrini et al. (1995). *Dinophysis acuminata* cells, concentrated in the upper portion of the cylinders, were siphoned out and individually isolated with microcapillary pipettes under 25X and 100 X microscope magnification. Each cell was transferred two to three times to slides with filtered-sterilized seawater (0.2 µm Millipore filters, Millipore Corp. Bedford, MA) and finally placed (individual cells and groups of 5 cells) in culture-plate wells of 0.2 mL containing 150 µL of either filtered seawater (FSW) from the same depth of collection (control) or the same water enriched with dissolved organic matter of M.W.>1 kD (DOM>1 kD) to a final concentration 50 times higher than the background level. Incubations were examined daily to record the number of cells on each well.

Estimates of division rates (µ) were obtained according to:

$$\mu = \frac{\ln N_f - \ln N_0}{t} \qquad (1)$$

Where µ (d^{-1}) is the specific division rate, N_f and N_0 are the final and initial cell numbers (cell/well) and t the time (d).

2.6 The model

The MARS3D hydrodynamical model (Lazure and Dumas, 2008) for the Northern Bay of Biscay was used to simulate the hydrodynamics in the study area. Model simulations extended from the French coast to 8ºW and from the Northern Spanish coast

to Southern England. The horizontal mesh size used had a resolution of 4 km, and 30 vertical levels were considered with a finer resolution near the surface. The simulation was forced by real conditions of tide, river run-off, heat fluxes and wind using data from the Arpège model of the French Met Office. Spin up from one year (2005) was considered.

A Lagrangian individual-particle tracking 3D-model—Ichthyop (Lett et al., 2008)—was used to simulate the possible advection or dispersion of virtual *Dinophysis* populations in the study area. Environmental conditions (3D field of currents, temperature and salinity) between 15 June and 30 July were provided by archived simulations of MARS3D configured for the Northern Bay of Biscay. In the Bay of Vilaine (BV), two areas were defined, Area 1, which extended from 47.8º N to 47.2º N and from -2.8º E to -2.1º E and roughly corresponds to station 31 from the first leg of the cruise (Fig 2) and Area 2, which represented the whole BV (Fig 1), from 46.7ºN to 47.8ºN and from 2º W to 3.3º W. Virtual particles movement was defined as a passive Lagrangian transport.

In this work, two sets of simulations were carried out. In the first set, each simulation consisted of a random release of 5000 particles representing virtual cells of *Dinophysis* within Area 1 every 5 days from 15 June to 30 July (0-20 m). Each simulation lasted 10 days. The proportion of particles retained was estimated every 2 m depth from surface (0 m) to 20 m. Particles were considered to be retained at the end of each simulation if they were still present in Area 1 or Area 2.

In the second set, Ichthyop simulations were used to evaluate the trajectory and the retention-dispersion pattern of 1000 virtual particles, from 9 to19 July, at 2-5 m depth, i.e.

253 the depth range where *D. acuminata* cells were detected during the first leg of the survey
254 (see section 3.5).
255
256 **3. Results**
257 *3.1 Seasonal distribution of* Dinophysis *during 2006*
258 The seasonal occurrence of *Dinophysis* spp. in the BV in 2006 showed a rather wide
259 temporal distribution. The *Dinophysis* growth season as defined in Xie et al. (2007)
260 started by the end of April (Fig 3) and two weeks later, on 15 May 2006, *Dinophysis*
261 populations reached 2300 cell L^{-1}. The bloom lasted until the end of July and the highest
262 cell density (6200 cell L^{-1}) was recorded on 19 June 2006. Therefore, the cruise (05-22
263 July) was carried out two weeks after the seasonal maximum and when *Dinophysis*
264 numbers were decreasing.
265
266 *3.2* Dinophysis *spp. distribution during the cruise*
267 During the first leg of the cruise (06-12 July), concentrations of *Dinophysis* spp. were
268 extremely low (< 50 cells L^{-1}) offshore but higher values (up to 500 cells L^{-1}) were found
269 in the River Loire and Vilaine plumes at stations with a high particle load, lower surface
270 salinity and steep vertical gradients of temperature (Fig 4, Fig 5). Sea surface temperature
271 (SST) estimated from satellite images presented a positive anomaly—in relation to a 22-y
272 (1986-2008) time series; courtesy of Nausicaa, IFREMER)—of 2.98ºC on 12 July (Fig
273 6). Temperature values obtained from the CTD casts exceeded 19ºC at surface and
274 exhibited strong horizontal and vertical gradients along the study area (Fig 5B, 5E).

275 Vertical distribution of *D. acuminata* in BV showed that the population was located
276 between the surface and the beginning of the pycnocline (1-4 m depth; Table 2, Fig 5)
277 within a community dominated by other dinoflagellates (*Prorocentrum micans, Ceratium*
278 *fusus* and *Gonyaulax diacantha*). *D. acuminata* maxima were never found associated to
279 the chlorophyll a (Chl *a*) maxima. The maximum concentration (1002 cells L^{-1}) was
280 observed on station 31 at 2.25 m depth (T= 18.5ºC, S= 33.8 σ_t, F equiv. to 0.85 µg Chl *a*
281 L^{-1}) on 11 July (Fig 7). At this point, the phytoplankton community located at the Chl *a*
282 maximum (15 m; F=14.5 µg Chl *a* L^{-1}) was composed by a population of
283 *Chrysochromulina* sp. ($1.5x10^6$ cells L^{-1})—that developed into a dense thin layer during
284 the second leg of the cruise—a diatom assemblage that comprised a mixture of
285 *Leptocylindrus danicus*, *L. minimus* and medium-sized *Chaetoceros* spp. (< $2x10^5$ cell
286 L^{-1}) and a dinoflagellate assemblage dominated by *Prorocentrum* spp. and ecdysal cysts
287 of *Fragilidium* spp. (ca. 5000 cell L^{-1}).
288 The horizontal distribution of *D. acuminata* during the second leg of the cruise (13-22
289 July) (Fig 8) shows that unlike during the first leg, concentrations of *D. acuminata* during
290 this period were very low (< 100 cells L^{-1}) in the whole study area.
291
292 *3.3 On board observations of* D. acuminata
293 No parasites were seen in any of the live samples observed by epifluorescence.
294 Most *D. acuminata* cells in FDA-treated samples appeared to be in good condition, with
295 branched, brightly autofluorescent (orange) chloroplasts. The frequency of viable cells
296 was higher than 89% in all samples (8) analyzed. Therefore, a predominance of green-

297 fluorescing metabolically-active cells was observed although some non metabolically-
298 active cells with weak red v or no fluorescence at all were also found (Fig 9).
299
300 *3.4 Short-term incubations with DOM enrichments.*
301 Individually picked cells of *D. acuminata* incubated in the well-plates showed a
302 positive growth, both in the filtered seawater controls and in the wells enriched with
303 concentrated DOM. Until day 4, *D. acuminata* cell-numbers increased in the controls and
304 in the DOM-enriched both experimental treatments in a similar manner, but from day 5
305 onwards, cells in the control wells stopped dividing, whereas those in the DOM-enriched
306 treatment continued division until the end of the experiment (day 7; Fig 10).
307 However, in comparison with the controls (max. 0.10 d^{-1}), cells incubated in DOM-
308 enriched water exhibited a significantly higher division rate (up to 0.23 d^{-1}) (Fig 10).
309
310 *3.4 Other biological observations*
311 An interesting observation during the first leg of the cruise was the frequent detection of
312 *Fragilidium* spp., at times the dominant or co-dominant microplanktonic species at the
313 depth of the chlorophyll- or the particle maximum. Probably due to the stress of
314 concentration procedures, cells appeared mainly as ecdysal cysts. After dissection of
315 individual specimens, a new species of *Fragilidium—F. duplocampanaeforme—*was
316 described and observed to contain preyed cells of *D. acuminata* (Nézan and Chomérat,
317 2009).
318
319 *3.5 Modelling simulations*

Results from the Ichthyop model simulations showed that, on average, particle-retention on Area 1 increased with depth, from 0-10% at a releasing depth of 0-10 m to 40-50% at 20 m (Fig 11A). The deeper the particles were released, the more retention over the Area 1 was observed (Fig 11A). The estimated retention in this Area was higher from 25 June to 5 July and from 15 to 30 July. In contrast, minimum values of retention were observed at 0-5 m depth on 20 June and 10 July. These simulations showed that less than 10% of the particles would be retained in Area 1 after 5 days, between 20 and 25 June.

Field observations showed that maximum concentrations of *D. acuminata* were found in Area 1 on 19 June and 11 July. On average, retention of particles released in the upper layer 0-5 m—the depth range where *D. acuminata* populations were detected—in Area 1 was maximal on 25 June-05 July and minimal on 20-25 June and 10-15 July (Fig 11). This retention pattern may explain the *D. acuminata* maxima found in the study area during the survey and its later dispersion and disappearance (Fig 3, Fig 8).

In contrast, although the minimum-retention periods in the whole BV region (Area 2; Fig 11B) coincided with those found in Area 1, the proportion of retained particles in Area 2 (35%) was much higher than in the estimations for Area 1 (5%). Therefore, although dispersed in a larger area, the virtual population of *Dinophysis* still remained in the BV after each simulation, even during high-dispersion periods.

The Ichthyop model was also used to simulate the retention-dispersion of the *D. acuminata* maximum found at station 31 (2-5 m depth; Fig 12). Retention rates decreased after 11 July and the particle population was advected southwardly immediately after their release (Fig 12). These results agree with the distribution of *D. acuminata* found during the second leg of the cruise.

4. Discussion

The growing season of *D. acuminata*—defined to occur from April to September in the BV (Xie et al., 2007)—started by the end of April in 2006, but finished unusually early, by the end of July, i.e. one month after reaching its seasonal cell maximum (19 June). Although high concentrations (>10^3 cell L^{-1}) of *Dinophysis* spp. were not found during the cruise, substantial information on the conditions associated with the bloom decline and the physiological status of *D. acuminata* was gathered.

Division rates of *D. acuminata* estimated from short-term incubations in culture-plate wells with addition of DOM (> 1 kD) to the local seawater were significantly higher than those from the control-wells with only local seawater. These results suggest a beneficial effect of DOM on *Dinophysis* growth that would explain the frequent co-occurrence of *D. acuminata* cell maxima with those of organic aggregates (Lunven et al., 2005). Maximum values of μ (0.23 d^{-1}) were 2-4 times lower than those observed under optimum culture conditions of *D. acuminata* fed on the ciliate *Myrionecta rubra* (= *Mesodinium rubrum*) by Park et al., 2006; Riisgaard and Hansen, 2009. These authors concluded that *Dinophysis* is an obligate mixotroph that requires both light and live prey for long term survival. Nevertheless, the enhanced growth observed in the DOM-enriched incubations suggests that DOM may act as a nutritional supplement that helps to maintain and even to increase population numbers between successive feedings on *Myrionecta*.

The high frequency of viable cells, the moderate division rates observed on the on board incubations and the healthy appearance of the cells observed immediately after

365 samples recollection indicates that the *D. acuminata* population under study was in good
366 physiological conditions.

367 The decline of dinoflagellate blooms has been thought to result from a combination of
368 physical and biological factors (Steidinger, 1973; Garcés et al., 1999). Amongst the
369 biological processes, sexual reproduction and encystment, aging of the population and
370 grazing have been identified as potential key factors to understand the bloom decline
371 (Calbet et al., 2003). Amongst the potential physical factors, changes in wind velocity
372 and direction, turbulence and mixing may also account for the decline of a dinoflagellate
373 population.

374 The importance of water transport in the population dynamics of *Dinophysis* spp. and
375 its possible advection to the coast has been described in several studies (i.e. Belgrano et
376 al., 1999; Delmas et al., 1992). Physical driving forces, such as wind and/or currents that
377 provoke accumulation-dispersion of *Dinophysis* cells have been already reported by some
378 authors (Koike et al., 2001; Koukaras and Nikolaidis, 2004; Soudant et al., 1997). More
379 recently, *Dinophysis* events have been related to the onshore transport of an eddy, located
380 offshore in the BV (Xie et al., 2007), that may constitute a retention area or "incubator"
381 for *D. acuminata*. Xie et al. (2007) related increased densities of *Dinophysis* spp. to
382 retentive zones where horizontal dispersion of the growing population was limited.
383 Soudant et al. (1997) explained *D. acuminata* abundance in Antifer (Normandy, France)
384 using a dynamic linear regression. They concluded that the disappearance of *D.*
385 *acuminata* cells in the area was mainly driven by northeasterly winds that provoked cells
386 dispersion and by increased tidal coefficients that induced *D. acuminata* dispersal by
387 dilution and water- masses movement. Our results from Ichthyop simulations favour the

388 consideration of these retention-dispersion patterns, since simulations of minimum
389 particle retention coincided with the disappearance of the *D. acuminata* peaks on 19 June
390 (REPHY data; Fig 4) and on 11 July (Cruise data; Fig 5). Moreover, maximum
391 percentages of particle dispersion were found at the surface, where the *D. acuminata* cell
392 maxima were observed (Table 2) during the cruise.

393 High dilution rates promoted by sea currents can be expected to return dinoflagellate
394 populations to earlier developmental phases or even disperse them completely (Zingone
395 and Wyatt, 2004). Results from Ichthyop show that although *D. acuminata* may have
396 been dispersed from its bloom location (Area 1), a percentage (10 %) of the population
397 remained in the whole BV (Area 2). Those cells still present in the area may have acted
398 as the seed for the next *D. acuminata* peak detected after the cruise by REPHY (Fig 4)
399 before their definitive disappearance at the beginning of August 2006.

400 Biological processes (i.e. plankton behaviour, grazing, growth, and mortality) can be
401 important factors that may influence the outcomes of 3D LPTM. The grazing impact of
402 zooplankton has been identified as a significant loss factor that could affect HABs
403 dynamics (Turner and Anderson, 1983; Watras et al., 1985). Grazing from protist such as
404 heterotrophic dinoflagellates and ciliates has been shown to cause considerably mortality
405 (< 50%) of even collapse of dinoflagellate blooms (Kamiyama et al., 2001; Kamiyama
406 and Matsuyama, 2005; Matsuyama et al., 1999). Following dissection of specimen from
407 samples collected during our cruise, Nézan and Chomérat (2009) observed that cells of
408 the heterotrophic dinoflagellate, *Fragilidium duplocampanaeforme*, often contained theca
409 of *D. acuminata* in their interior. The unusual high concentrations of ecdysal cysts of
410 *Fragilidium* observed during the first leg of the cruise combined with the moderate

411 concentrations of *Dinophysis* may have caused a high grazing impact of the former in the
412 *D. acuminata*.

413 There are other interactions between organisms, different from predator-prey
414 relationships that may have a strong impact on the population dynamics of harmful algae.
415 In this context, allelopathy has been considered as a potential agent that could promote
416 bloom decline and as a key factor in the control of algal succession. Among others, the
417 allelopathic effects of *Chrysochromulina polylepis* on several plankton species include an
418 initial decrease in growth rate of the tested algae, followed by a decline in their
419 population numbers (Schmidt and Hansen, 2001). In our study, the decline of *D.*
420 *acuminata* was observed coinciding with the onset of a *Chrysochromulina* sp. bloom that
421 formed a conspicuous thin layer (10 m depth) during the second leg of the cruise.

422 Parasitism is also recognized as an important microbial control of bloom-forming
423 dinoflagellates, with species of *Amoebophrya* being particularly noteworthy, as they are
424 widely distributed in coastal environments and infect numerous host taxa, including
425 several toxin-producing species (Park et al., 2004). Recently, *D. acuminata* has been
426 reported to be one of the many hosts for *Amoebophrya* spp. (Salomon et al., 2009;
427 Gonzalez-Gil et al., accepted) and for that, especial attention was paid to detect infected
428 *D. acuminata* cells during the survey. Although epidemic outbreaks of *Amoebophrya* spp.
429 have been reported for several dinoflagellate species, such as *Alexandrium catenella*
430 (Nishitani et al., 1985; Taylor, 1968), *Ceratium falcaltiforme* (Salomon et al., 2009) and
431 *D. norvegica* (Salomon et al., 2003), .*D. acuminata* has not shown high infection levels in
432 field studies (1-3 %, Gonzalez-Gil et al., Personal communication). During this study,

433 frequencies of infected cells were below detection limits and parasites, at least in this
434 situation, can be discarded as a relevant loss factor

435 The relationship between *Dinophysis* and environmental factors has been extensively
436 considered in many studies (reviewed in Maestrini, 1998). The summer 1983, defined in
437 Lassus et al. (1985) as a very hot summer, *Dinophysis* populations were found between
438 15-21ºC in Southern Brittany coasts. The highest abundances during that year were
439 observed at 15ºC, and corresponded to the beginning of the population dispersal. Besides,
440 although large surface lenses of water of 24ºC were detected in southern Brittany in that
441 summer , *Dinophysis* spp. populations were only found within the BV, characterized at
442 that moment by moderate surface temperatures (below 18ºC). During the HABIT cruise
443 on July 2006, *D. acuminata* was mainly found near the surface, where the temperature
444 was significantly higher (19-20.51ºC) than the average typical summer conditions in the
445 area (Fig 7).

446 The effect of daily vertical migration (DVM) on retention and dispersion of *D.*
447 *acuminata* populations has not been taken into account in our model simulations, and
448 indeed, no signs of DVM of this species were observed during our cruise. However, *D.*
449 *acuminata* cells are not passive particles and some evidence has been presented for its
450 DVM under very calmed conditions in Ría de Vigo (Villarino et al., 1995). Nevertheless,
451 in other situations and in the same region, *D. acuminata* has not been observed to perform
452 any vertical migration M (Velo-Suárez et al., 2008; González-Gil et al., accepted). It
453 seems that DVM is not a constant feature in the behaviour of *D. acuminata*, and further
454 studies are needed to decide under which circumstances virtual particles should be
455 programmed to have DVM in model simulations.

Biological observations and analysis during the survey have emphasized the importance of biological processes in HABs population dynamics. However, the parameterization and calibration of these processes (i.e. mortalities induced by predation, allelopathy, and temperature effects, parasitism and swimming behaviour and buoyancy) are not a simple task and species-specific vital rates are needed to include them into individual based models and obtain accurate simulations of *D. acuminata* dynamics in the future.

The first application of a 3D LPTM with a HAB species shows how these models are able to reproduce well *D. acuminata* patches and dispersion patterns obtained in the field. Comparisons between survey data (*D. acuminata* concentrations) and model output (% of virtual particle retention) were in good agreement (Fig 4, Fig 8 and Fig 12), considering that an exact correspondence between model outputs and observations in a system with strong meso- and sub- mesoscale activity is difficult to achieve. Physical factors (wind-generated turbulence, advection, etc) can explain the rapid collapse of a HAB population but biological interactions cannot be dismissed during the decline processes. In order to understand the interactions in the pelagic environment, we need to integrate biology and physics on the temporal and spatial scales of the population dynamics of the individual species. Results from this work give confidence to set up, in a near future, a 3D LPTM of the dynamics of *D. acuminata* for the Northern Bay of Biscay that should include vertical migration patterns and other important biological aspects.

6. Acknowledgments

We thank the crew of *R/V* Thalassa for their help, M.M. Daniélou, E. Le Gall, A. Youenou and I. Ramilo for technical assistance, and Christian Béchemin for providing DOM concentrates. This work was funded by projects HABIT (EC 6FP, GOCE-CT-2005-003932) and TURDIRRIAS (CTM2006-13884-CO2-02/MAR). This is a contribution to the GEOHAB Core Research Project HABs and Stratification

7. References

Aminot, A., Kerouel, R., 2004. Hydrologie des écosystèmes marins. Paramètres et analyses. Collection Méthodes d'analyse en milieu marin. IFREMER, France.

Belgrano, A., Lindahl, O., Hernroth, B., 1999. North Atlantic Oscillation, primary productivity and toxic phytoplankton in the Gullmar Fjord, Sweden (1985-1996). Proc. Roy. Soc. Lond. B. Bio. 266, 425–430.

Benner, R., Biddanda, B., Black, B., McCarthy, M., 1997. Abundance, size distribution, and stable carbon and nitrogen isotopic compositions of marine organic matter isolated by tangential-flow ultrafiltration. Mar. Chem. 57, 243–263.

Calbet, A., Vaqué, D., Felipe, J., Vila, M., Sala, M. M., Alcaraz, M., Estrada, M., 2003. Relative grazing impact of microzooplankton and mesozooplankton on a bloom of the toxic dinoflagellate *Alexandrium minutum*. Mar. Ecol. Prog. Ser., 259, 303–309.

Coleman, N. K., Vestal, J. R., 1987. An epifluorescent microscopy study of enzymatic hydrolysis of fluorescein diacetate associated with the ectoplasmic net elements of the protist *Thraustochytrium striatum*. Can. J. Microbiol. 33, 841–843.

Delmas, D., Herbland, A., Maestrini, S. Y., 1992. Environmental conditions which lead to increase in cell density of the toxic dinoflagellates *Dinophysis* spp. in nutrient-rich and nutrient-poor waters of French Atlantic coast. Mar. Ecol. Prog. Ser. 89, 53–61.

504 Delmas, D., Herbland, A., Maestrini, S. Y., 1993. Do *Dinophysis* spp. come from the
505 "open sea" along the French Atlantic coast? in: Smayda, T., Shimizu, Y. (Eds.),
506 Toxic phytoplankton blooms in the sea. Elsevier, Amsterdam, pp. 489–494.

507 Dodson, A. N., Thomas, W. H., 1978. Reverse filtration, in: Sournia, A. (Ed.),
508 Phytoplankton Manual. UNESCO, Paris, pp. 104–106.

509 Gallego, A., North, E. W., Petitgas, P., 2007. Introduction: status and future of modelling
510 physical-biological interactions during the early life of fishes. Mar. Ecol. Prog.
511 Ser. 347, 122–126.

512 Garcés, E., Masó, M., Camp, J., 1999. A recurrent and localized dinoflagellate bloom in a
513 Mediterranean beach. J. Plankton Res. 21, 2373–2391.

514 Gentien, P., 1986. A method for evaluating phytoplankton viability by induced
515 fluorochromasia, in: Manzoli, F. A. (Ed.), Progress in flow cytometry. ISBN 90-
516 9001361-X, pp. 151–164.

517 Gentien, P., Lunven, M., Lehatre, M., Dunvent, J. L., 1995. *In situ* depth profiling of
518 particles sizes. Deep Sea Res. I 42, 1297–1312.

519 González-Gil, S., Velo-Suárez, L., Gentien, P. Ramilo, I., Reguera , R., accepted.
520 Phytoplankton assemblages and characterization of *Dinophysis acuminata*
521 population during an upwelling-donwelling cycle. Aquat. Microb. Ecol.

522 Guo, L., Coleman, C. H. J., Santschi, P. H., 1994. The distribution of colloidal and
523 dissolved organic carbon in the Gulf of Mexico. Mar. Chem. 45, 105–119.

524 Kamiyama, T., Matsuyama, Y., 2005. Temporal changes in the ciliate assemblage and
525 consecutive estimates of their grazing effect during the course of a *Heterocapsa*
526 *circularisquama*. J. Plankton Res. 27, 303–311.

527 Kamiyama, T., Takayama, H., Nishii, Y., Uchida, Y., 2001. Grazing impact of the field
528 ciliate assemblage on the bloom of the toxic dinoflagellate *Heterocapsa*
529 *circularisquama*. Plankton Biol. Ecol. 48, 10–18.

530 Kim, S., Kang, Y. G., Kim, H. S., Yih, W., Coats, D. W., Park, M. G., 2008. Growth and
531 grazing responses of the mixotrophic dinoflagellate *Dinophysis acuminata* as
532 functions of light intensity and prey concentration. Aquat. Microb. Ecol. 51, 301–
533 310.

534 Koike, K., Otobe, H., Takagi, M., Yoshida, T., Ogata, T., Ishimaru, T., 2001. Recent
535 occurrences of *Dinophysis fortii* (dinophyceae) in the Okkirai Bay, Sanriku,
536 Northern Japan, and related environmental factors. J. Oceanogr. 57, 165–175.

537 Koukaras, K., Nikolaidis, G., 2004. *Dinophysis* blooms in the Greek coastal waters
538 (Thermaikos Gulf, NW Aegean Sea). J. Plankton Res. 26, 445–457.

539 Lassus, P., Barduouil, M., Trunquet, I., Trunquet, P., Le Baut, C., Pierre, M. J., 1985.
540 *Dinophysis acuminata* distribution and toxicity along the Southern Brittany Coast
541 (France): correlation with hydrological parameters, in: Anderson, D. M., White,
542 A. W., Baden, D. G. (Eds.), Toxic Dinoflagellates. Elsevier Science Publishing,
543 Inc, pp. 159–164.

544 Lazure, P., Dumas, F., 2008. An external-internal mode coupling for a 3D
545 hydrodynamical model at regional scale (MARS). Adv. Wat. Res. 31, 233–250.

546 Lazure, P., Dumas, F., Vrignaud, C., 2008. Circulation on the armorican shelf (Bay of
547 Biscay) in autumn. J. Marine Syst. 72, 218–237.

548 Lazure, P., Jegou, A. M., 1998. 3D modelling of seasonal evolution of Loire and Gironde
549 plumes on Biscay Bay continental shelf. Oceanol. Acta 21, 165–177.

550 Lett, C., Verley, P., Mullon, C., Parada, C., Brochier, T., Penven, P., Blanke, B., 2008. A
551 Lagrangian tool for modelling ichthyoplankton dynamics. Environ. Modell.
552 Softw. 23, 1210–1214.

553 Lunven, M., Gentien, P., Kononen, K., Le Gall, E., Danielou, M. M., 2003. *In situ* video
554 and diffraction analysis of marine particles. Estuar. Coast. Shelf Sci. 57, 1127–
555 1137.

556 Lunven, M., Guillaud, J. F., Youenou, A., Crassous, M. P., Berric, R., Le Gall, E.,
557 Kerouel, R., Labry, C., Aminot, A., 2005. Nutrient and phytoplankton distribution
558 in the Loire River plume (Bay of Biscay, France) resolved by a new Fine Scale
559 Sampler. Estuar. Coast. Shelf Sci. 65, 94–108.

560 Maestrini, S. Y., 1998. Bloom dynamics and ecophysiology of *Dinophysis* spp, in:
561 Anderson, D. M., Cembella, A. D., Hallegraeff, G. M. (Eds.), Physiological
562 ecology of harmful algae blooms. Vol. NATO ASI, Series G of Ecological
563 Sciences 41. Springer, Berlin Heidelberg, New York, pp. 243–266.

564 Maestrini, S. Y., Berland, B. R., Grzebyk, D., Spano, A. M., 1995. *Dinophysis* spp. cells
565 concentrated from nature for experimental purposes, using size fractionation and
566 reverse migration. Aquat. Microb. Ecol. 9, 177–182.

567 Marcaillou, C., Gentien, P., Lunven, M., Grand, J. L., Mondeguer, F., Daniélou, M. M.,
568 Crassous, M., Youenou, P., 2001. *Dinophysis acuminata* distribution and specific
569 toxin content in relation to mussel contamination, in: Hallegraeff, G. M.,
570 Blackburn, S. I., Bolch, C. J., Lewis, R. J. (Eds.), Harmful Algal Blooms. IOC of
571 UNESCO, Paris, pp. 356–359.

572 Matsuyama, Y., Miyamoto, M., Kotani, Y., 1999. Grazing impacts of the heterotrophic
573 dinoflagellate *Polykrikos kofoidii* on a bloom of *Gymnodinium catenatum*. Aquat.
574 Microb. Ecol. 17, 91–98.

575 Nishitani, L., Erickson, G., Chew, K. K., 1985. Role of the parasitic dinoflagellate
576 *Amoebophrya ceratii* in control of *Gonyaulax catenella* populations, in:
577 Anderson, D. M., White, A. W., Baden, D. G. (Eds.), Toxic dinoflagellates.
578 Elsevier, New York, pp. 225–230.

579 Nézan, E., Chomérat, N., 2009. *Fragilidium duplocampanaeforme* sp. nov.
580 (Dinophyceae): A new phagotrophic dinoflagellate from the French Atlantic
581 coast. Eur. J. Protistol 45, 2–12.

582 Park, M. G., Kim, S., Kim, H. S., Myung, G., Kang, Y. G., Yih, W., 2006. First
583 successful culture of the marine dinoflagellate *Dinophysis acuminata* in cultures.
584 Aquat. Microb. Ecol. 45, 101–106.

585 Park, M. G., Yih, W., Coats, D. W., 2004. Parasites and phytoplankton, with special
586 emphasis on dinoflagellate infections. J. Eukaryot. Microbiol. 51, 146–155.

587 Purina, I., Balode, M., Béchemin, C., Põder, T., Verité, C., Maestrini, S., 2004. Influence
588 of dissolved organic matter from terrestrial origin on the chances of dinoflagellate
589 species composition in the Gulf of Riga, Baltic Sea. Hydrobiologia 514, 127-137.

590 Riisgaard, K., Hansen, P. J., 2009. Role of food uptake for photosynthesis, growth and
591 survival of the mixotrophic dinoflagellate *Dinophysis acuminata*. Mar. Ecol. Prog.
592 Ser. 381, 51–62.

593 Salomon, P. S., Graneli, E., Neves, M. H. C. B., Rodríguez, E. G., 2009. Infection by
594 *Amoebophrya* spp. parasitoids of dinoflagellates in a tropical marine coastal area.
595 Aquat. Microb. Ecol. 55 (2), 143–153.

596 Salomon, P. S., Janson, S., Graneli, E., 2003. Parasitism of *Dinophysis norvegica* by
597 *Amoebophrya* sp in the Baltic Sea. Aquat. Microb. Ecol. 33 (2), 163–172.

598 Santos, A. M. P., Chicharo, A., Dos Santos, A., Moita, T., Oliveira, P. B., Peliz, A., Re,
599 P., 2007. Physical-biological interactions in the life history of small pelagic fish in
600 the western iberia upwelling ecosystem. Prog. Oceanogr. 74 (2-3), 192–209.

601 Schmidt, L. E., Hansen, P. J., 2001. Allelopathy in the prymnesiophyte
602 *Chrysochromulina polylepis*: Effect of cell concentration, growth phase and pH.
603 Mar. Ecol. Prog. Ser. 216, 67–81.

604 Soudant, D., Beliaeff, B., Thomas, G., 1997. Explaining *Dinophysis* cf. *acuminata*
605 abundance in Antifer (Normandy, France) using dynamic linear regression. Mar.
606 Ecol. Prog. Ser. 156, 67–74.

607 Steidinger, K. A., 1973. Phytoplankton ecology: a conceptual review based on eastern
608 Gulf of Mexico research. CRC Rev. Microb. 3, 49–68.

609 Taylor, F. J. R., 1968. Parasitism of the toxin-producing dinoflagellate *Gonyaulax*
610 *catenella* by the endoparasitic dinoflagellate *Amoebophrya ceratii*. J. Fish. Res.
611 Board. Can. 25, 2241–2245.

612 Turner, J. T., Anderson, D. M., 1983. Zooplankton grazing during dinoflagellate blooms
613 in a Cape Cod embayment, with observations of predation upon tintinnids by
614 copepods. Mar. Ecol. 4, 359–374.

615 Utermöhl, H., 1931. Neue wege in der quantitativen Erfassung des Planktons (mit
616 besonderer Berücksichtigung des Ultraplanktons). Verh. Int. Ver. Theor. Angew.
617 Limnol. 5, 567–596.

618 Velo-Suárez, L., González-Gil, S., Gentien, P., Lunven, M., Bechemin, C., Fernand, L.,
619 Raine, R., Reguera, B., 2008. Thin layers of *Pseudo-nitzschia* spp. and the fate of
620 *Dinophysis acuminata* during an upwelling-downwelling cycle in a Galician Ría.
621 Limnol. Oceanogr. 53, 1816–1834.

622 Velo-Suárez, L., Reguera, B., Garces, E., Wyatt, T., 2009. Vertical distribution of
623 division rates in coastal dinoflagellate *Dinophysis* spp. populations: implications
624 for modelling. Mar. Ecol. Prog. Ser. 385, 87–96.

625 Villarino, M. L., Figueiras, F. G., Jones, K. J., Álvarez-Salgado, X. A., Richard, J.,
626 Edwards, A., 1995. Evidence of *in situ* diel vertical migration of a red-tide
627 microplankton species in Ría de Vigo (NW Spain). Mar. Biol. 123, 607–617.

628 Watras, C. J., Garcon, V. C., Olson, R. J., Chisholm, S. W., Anderson, D. M., 1985. The
629 effect of zooplankton grazing on estuarine bloom of the toxic dinoflagellate
630 *Gonyaulax tamerensis*. J. Plankton Res. 7, 891–908.

631 Xie, H., Lazure, P., Gentien, P., 2007. Small scale retentive structures and *Dinophysis*. J.
632 Marine Syst. 64, 173–188.

633 Yasumoto, T., Murata, M., Oshima, Y., Sano, M., Matsumoto, G. K., Clardy, J., 1985.
634 Diarrhetic shellfish toxins. Tetrahedron 41 (6), 1019–1025.

635 Zingone, A., Wyatt, T., 2004. Harmful Algal Blooms: Keys to the understanding of
636 phytoplankton ecology, in: Robinson, A. R., Brink, K. H. (Eds.), The Global
637 Coastal Ocean: Multi-Scale Interdisciplinary Processes. The Sea, Volume 13.
638 Harvard University Press, pp. 867–926.

639

Fig 1: (A) Map of Western Europe and location of the Northern Bay of Biscay (B) Location of the Bay of Vilaine (BV) in the Northern Bay of Biscay.

Fig 2: Spatial distribution of sampling sites in the Northern Bay of Biscay during the first (A) and the second leg (B) of the HABIT 2006 survey.

Fig 3: Weekly distribution of *Dinophysis* spp. for 2006 in the BV (Data from REPHY). The extension of the *Dinophysis* season is highlighted with an arrow and the period when HABIT2006 cruise was carried out is marked as a shadowed area.

Fig 4: (A) Horizontal distribution of *D. acuminata* cell maxima in the Northern Bay of Biscay during the first leg of the survey (06-12 July 2006). (B) Detail of the *D. acuminata* horizontal abundance in the BV (06-12 July 2006).

Fig. 5: Horizontal distribution of (A) salinity, (C) temperature and (E) particle load measured with the IPSAP profiler in the study area from 06-12 July. Triangles in A, C and E indicate sampling points during the first leg. Vertical distribution of (B) salinity, (D) temperature and (F) particle load along a transect off the Loire estuary (shown as a line in panel A). *D. acuminata* maxima (cell L^{-1}) and their location in the water column are also marked in panels B, D, and F.

Fig. 6: Distribution of sea surface temperature (SST) anomalies at the Northern Bay of Biscay on 12 July 2006 (EUMETSAT). Average SST was obtained from a 22-yr time series (1986-2008).

663 **Fig. 7**: Vertical distribution of *D. acuminata* at station 31 (BV) on 11 July 2006.

664

665 **Fig. 8**: (A) Horizontal distribution of *D. acuminata* cell maxima in the Northern Bay of
666 Biscay during the second leg of the survey (13-22 July 2006). (B) Detail of the horizontal
667 distribution of *D. acuminata* in the BV (13-22 July 2006).

668

669 **Fig. 9**: An FDA-treated field sample. (A) The black arrow indicates metabolically-active
670 cell of *D. acuminata* in DIC micrograph, and (B); yellow arrow indicate non
671 metabolically-active cells with weak fluorescence or with no fluorescence at all.

672

673 **Fig. 10**: Incubations (5 cell well^{-1}) of *D. acuminata* with and without enrichment with
674 DOM>1 kD from BV. Moderate growth: μ_{max}= 0.23 d^{-1} (0.33 div d^{-1}) was observed in
675 DOM-enriched wells.

676

677 **Fig. 11** Percentages of retained particles obtained from Ichthyop runs in the BV from 15
678 June to 30 July 2006 in (A) Area 1 (sta 31) and (B) the whole BV. Plot shaded areas mark
679 when *D. acuminata* reached its maximum concentration (data on 19 July from REPHY
680 and on 11 July from cruise) in the BV.

681

682 **Fig. 12** Results from Ichtyop transport scenarios from 09 July to 19 July at 2-5 m depth.
683 (A) Map of the Northern Bay of Biscay showing Area 2. Position of particles after (B) 2-
684 day, (C) 4-day, (D) 6-day, (E) 8-day, and (F) 10-day simulation are shown as black dots.
685 Red box indicates the location of Area 1.

Table 1: Temporal distribution of sampling sites in the Northern Bay of Biscay during the first and the second leg of the HABIT 2006 survey.

Leg 1		**Leg 2**	
Date (July)	Sampling stations	Date (July)	Sampling stations
06	1-4	13	38
07	5-10	14	39-41
08	11-15	15	42-45
09	16-21	16	47
10	22-28	18	58-60,62-63
11	29-33	19	64-68
12	34-37	20	71
		21	75,77
		22	78-79

Table 2: Depth of *D. acuminata* cell maxima at each station where its concentration in the whole water column reached 100 cells L^{-1} during the first leg of the cruise (06-12 July).

Station	Day	Sampling hour (GMT)	*D. acuminata* cells L^{-1}	Depth (m)
8	07 July	12:30	304	7
9	07 July	15:30	148	1.7
20	09 July	21:00	933	4
21	09 July	23:30	707	4
23	10 July	04:00	603	16
26	10 July	01:00	487	1
31	11 July	12:30	1002	2.25
37	12 July	12:00	632	2

Figure 1

Click here to download high resolution image

Click here to view linked References

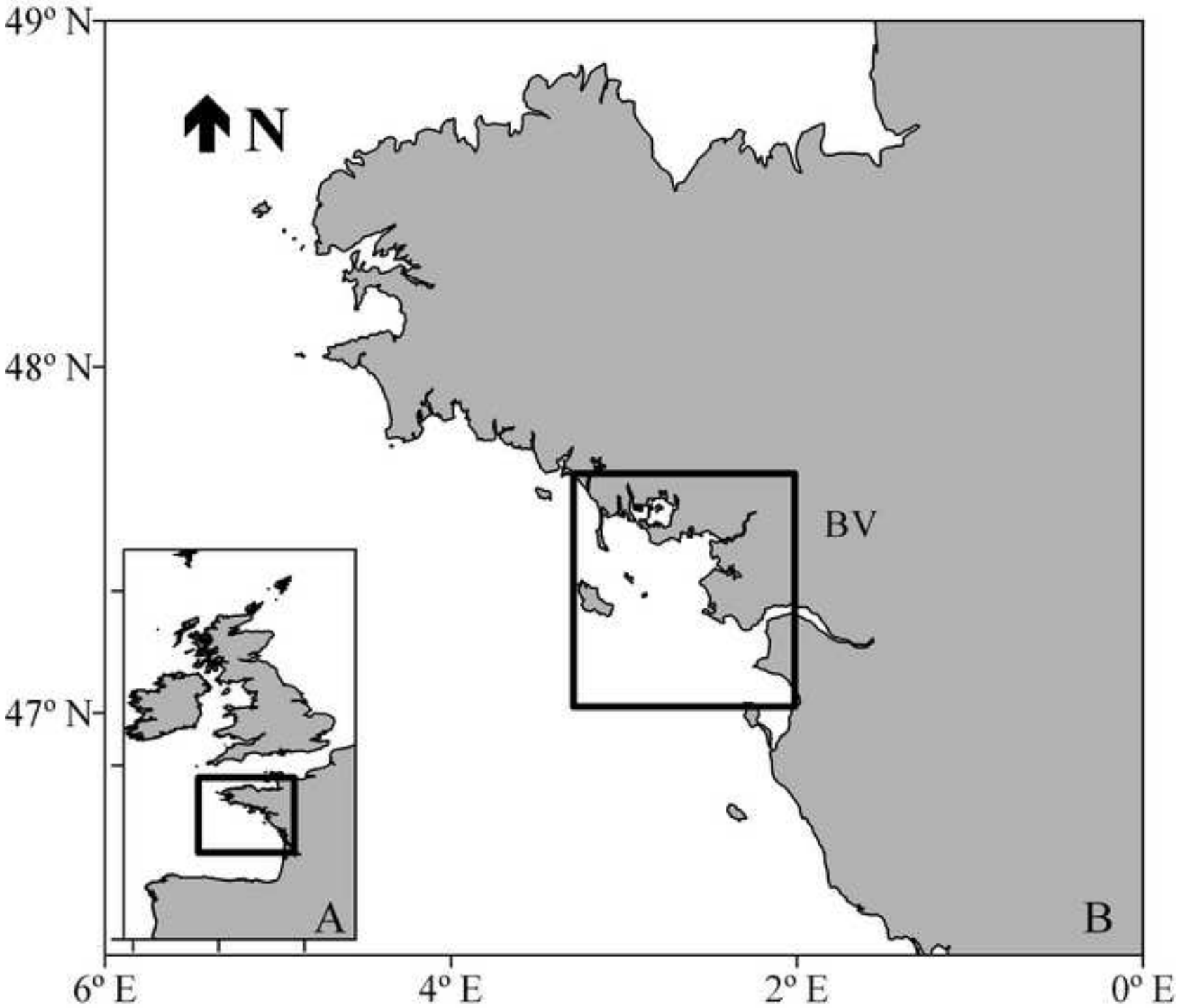

Figure 2

Click here to download high resolution image

Click here to view linked References

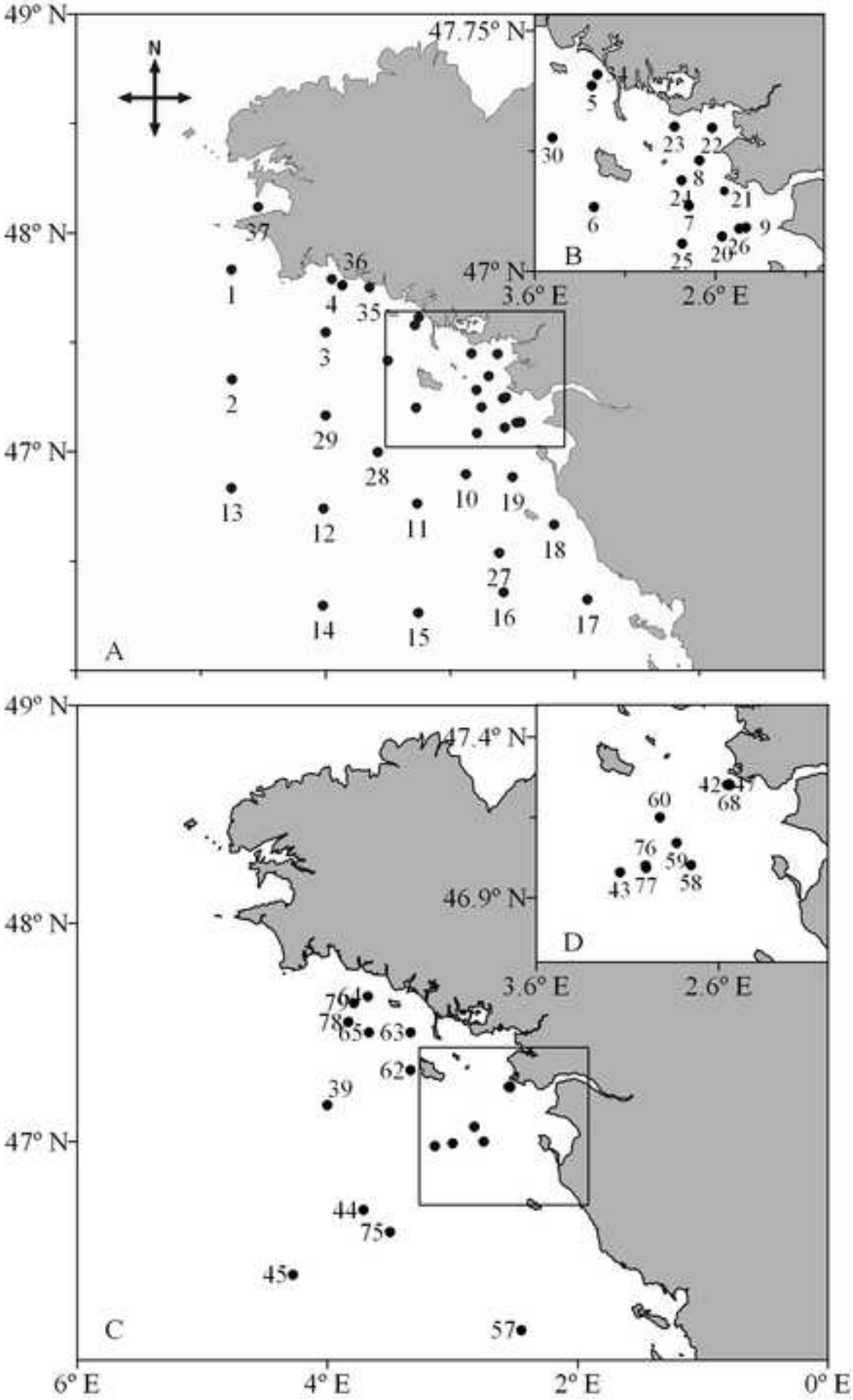

Figure 3

Click here to download high resolution image

Click here to view linked References

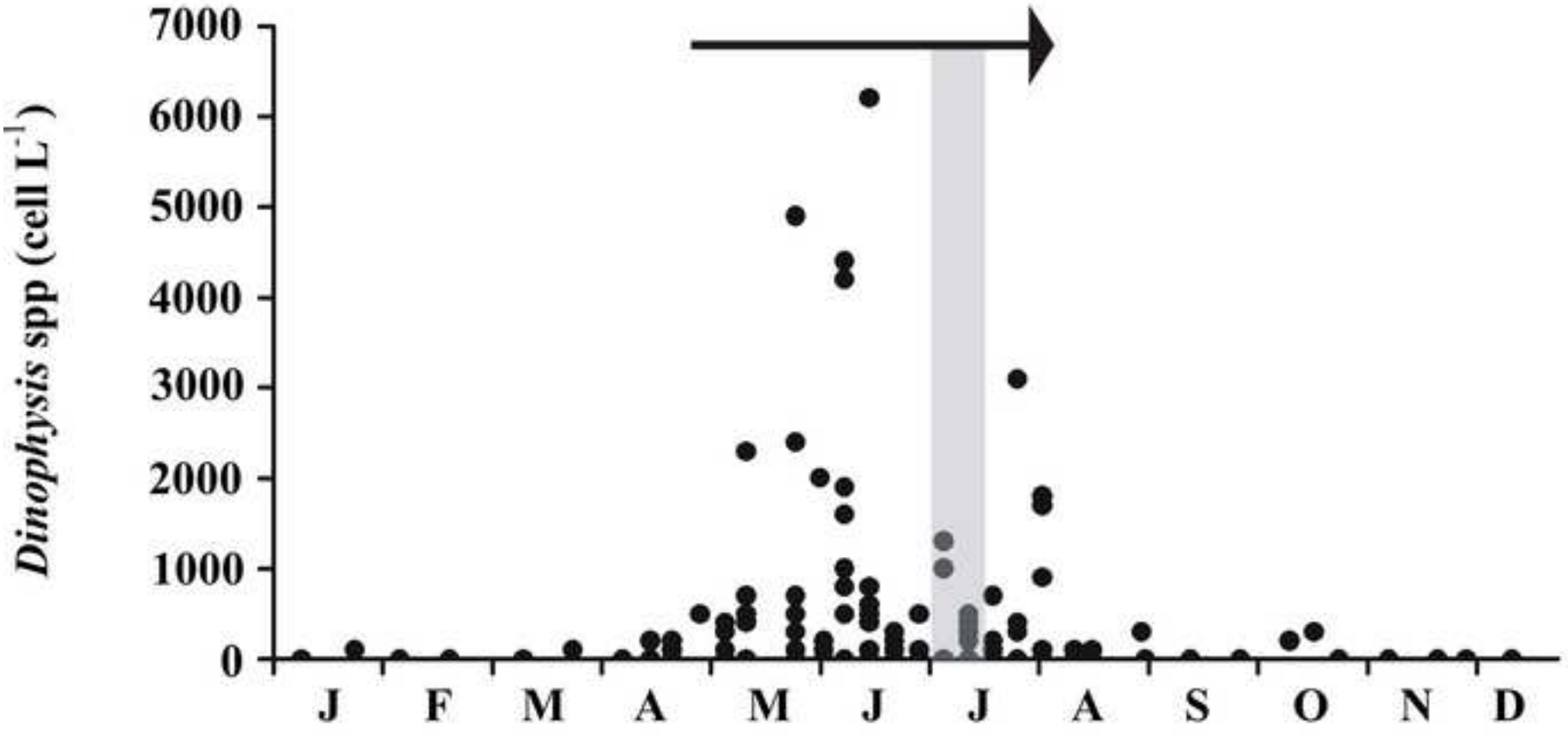

Figure 4

Click here to download high resolution image

Click here to view linked References

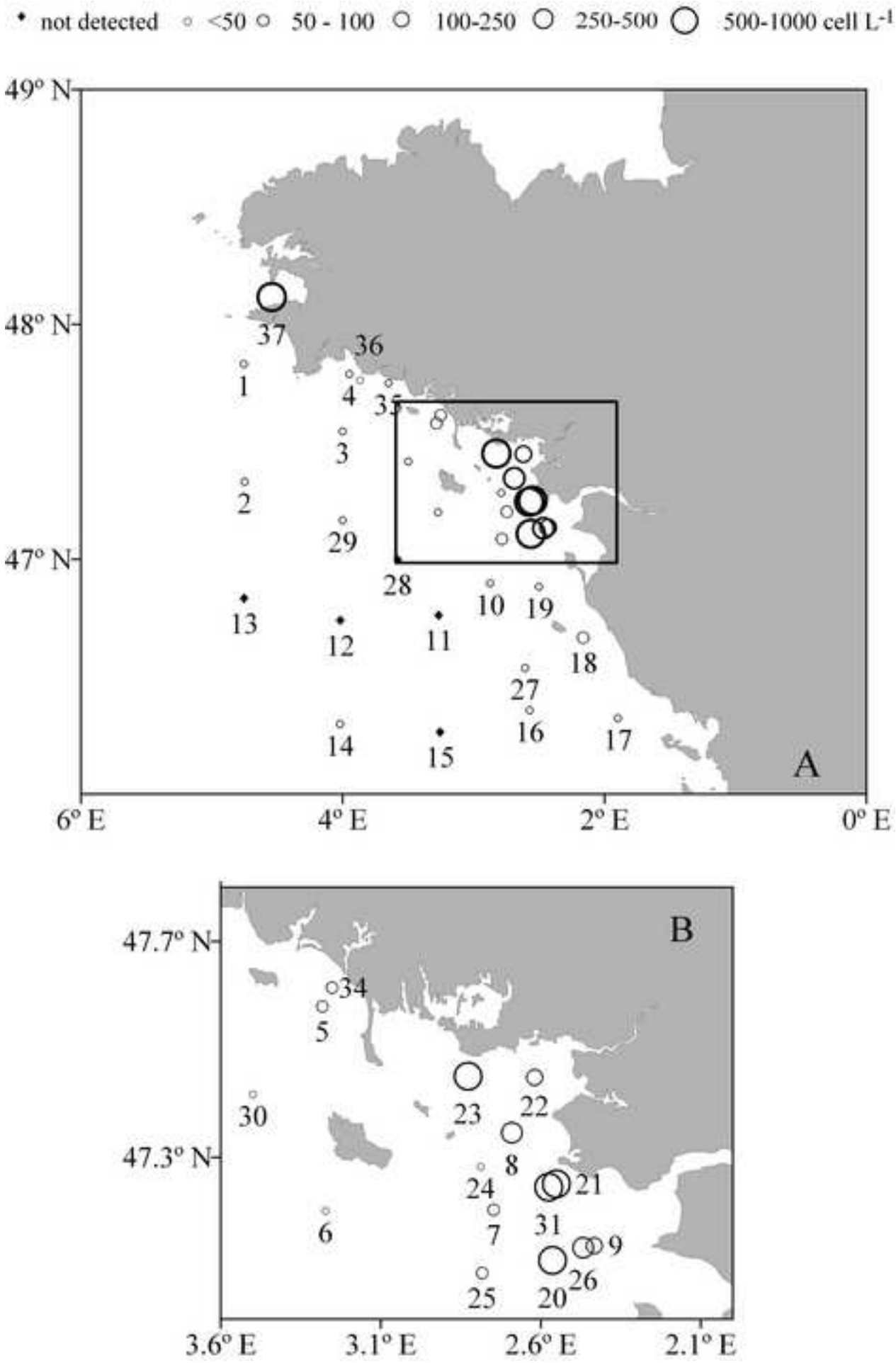

Figure 5

Click here to download high resolution image

Click here to view linked References

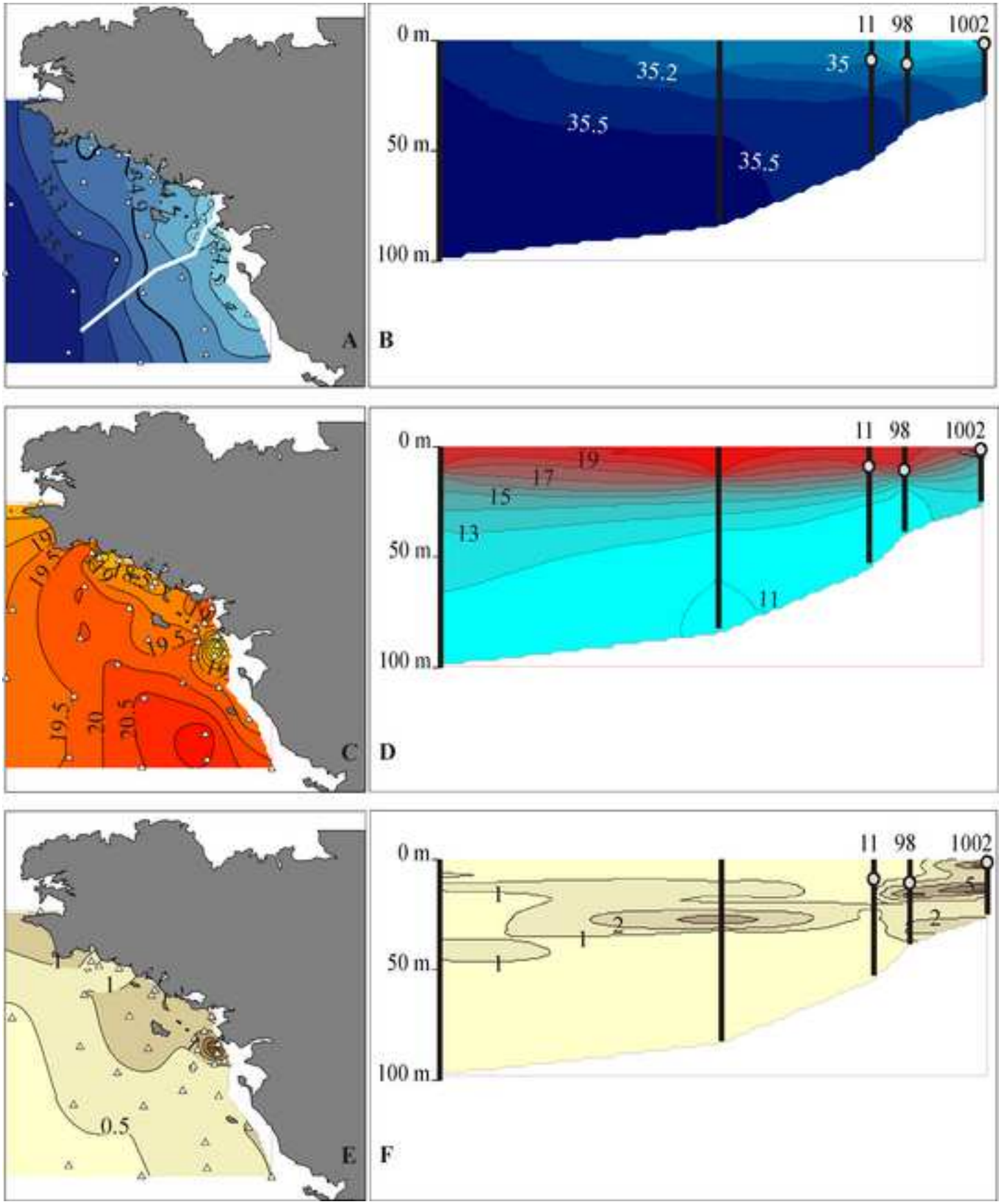

Figure 6

Click here to download high resolution image

Click here to view linked References

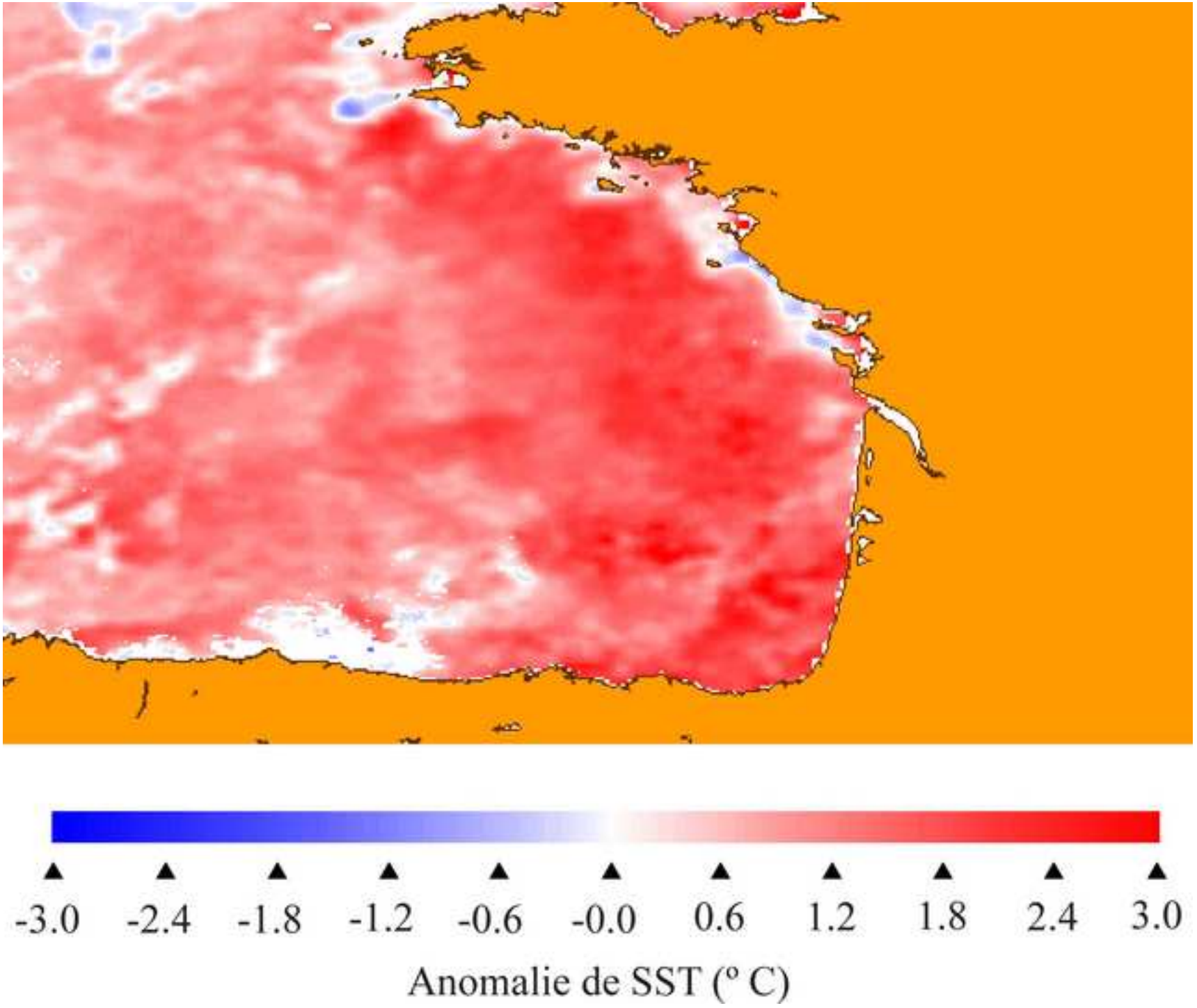

Figure 7

Click here to download high resolution image

Click here to view linked References

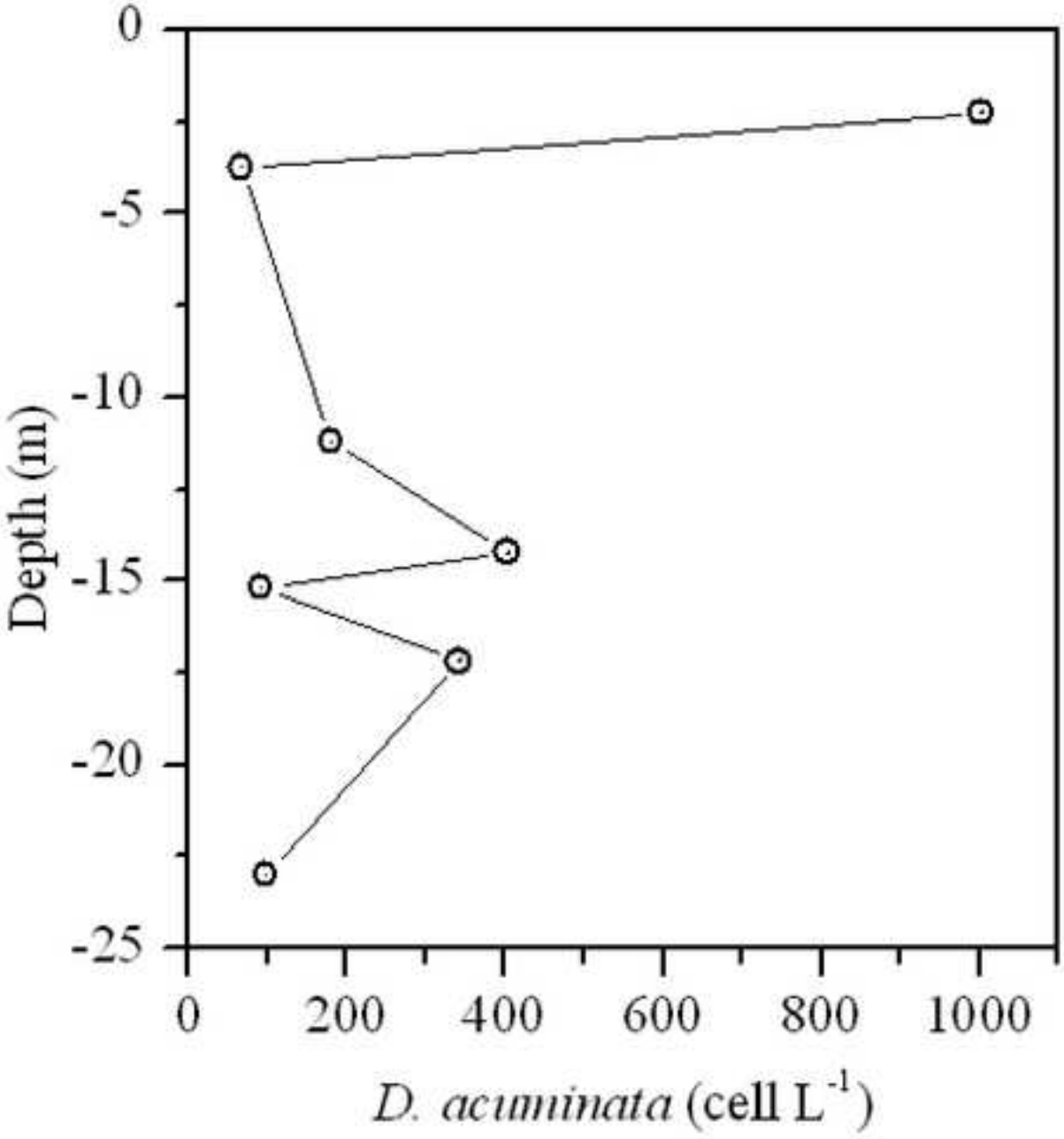

Figure 8

Click here to download high resolution image

Click here to view linked References

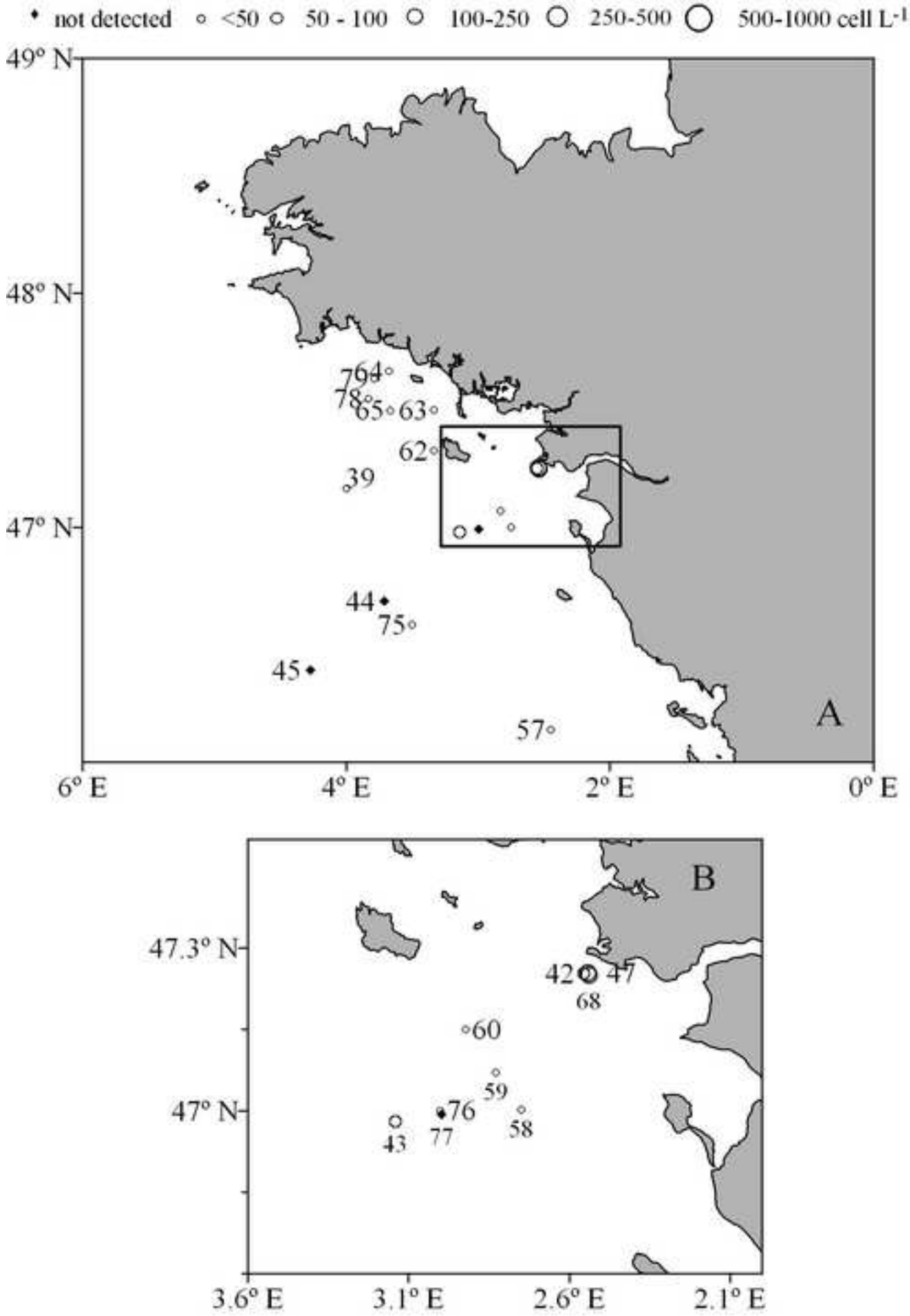

Figure 9

Click here to download high resolution image

Click here to view linked References

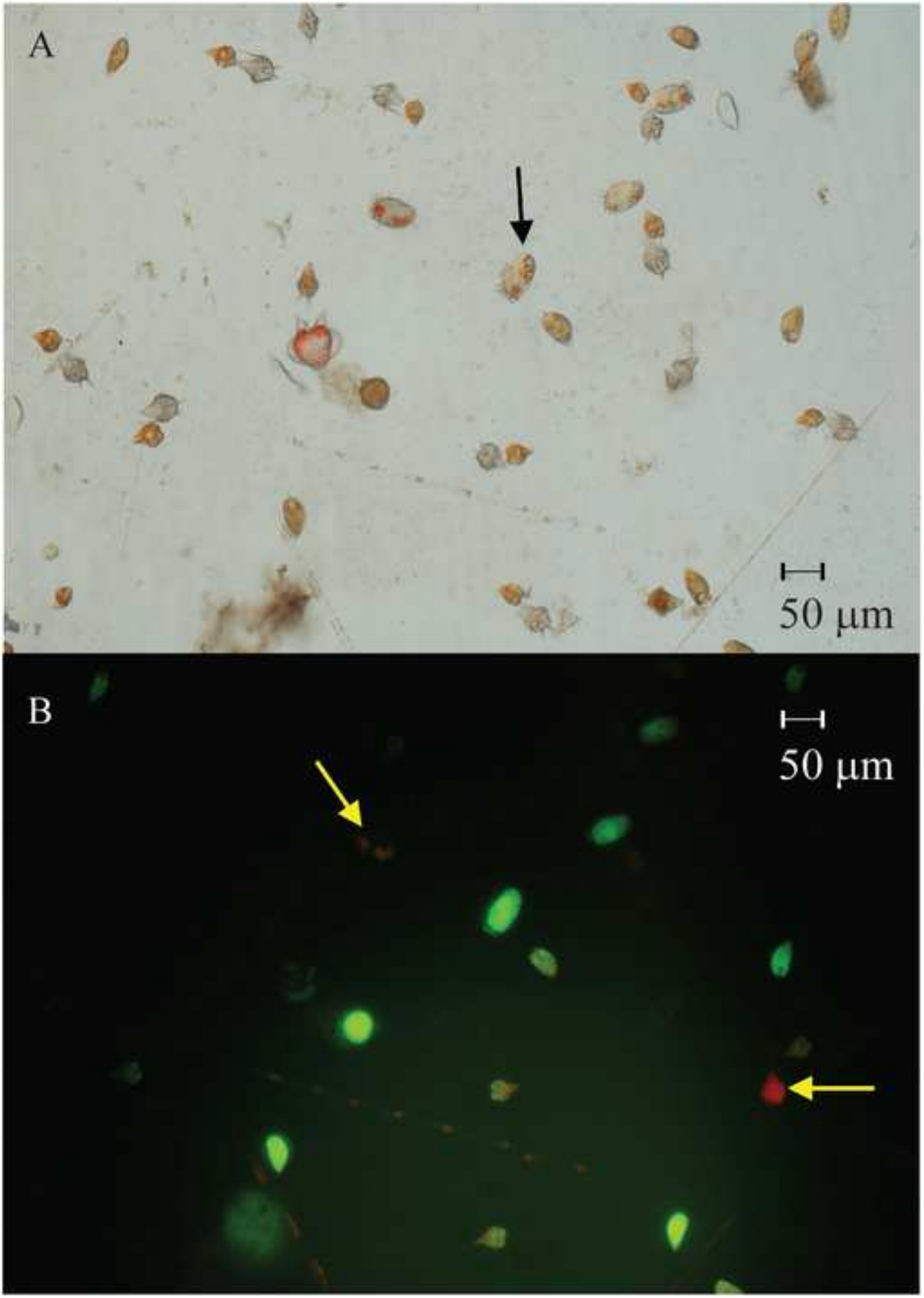

Figure 10

Click here to download high resolution image

Click here to view linked References

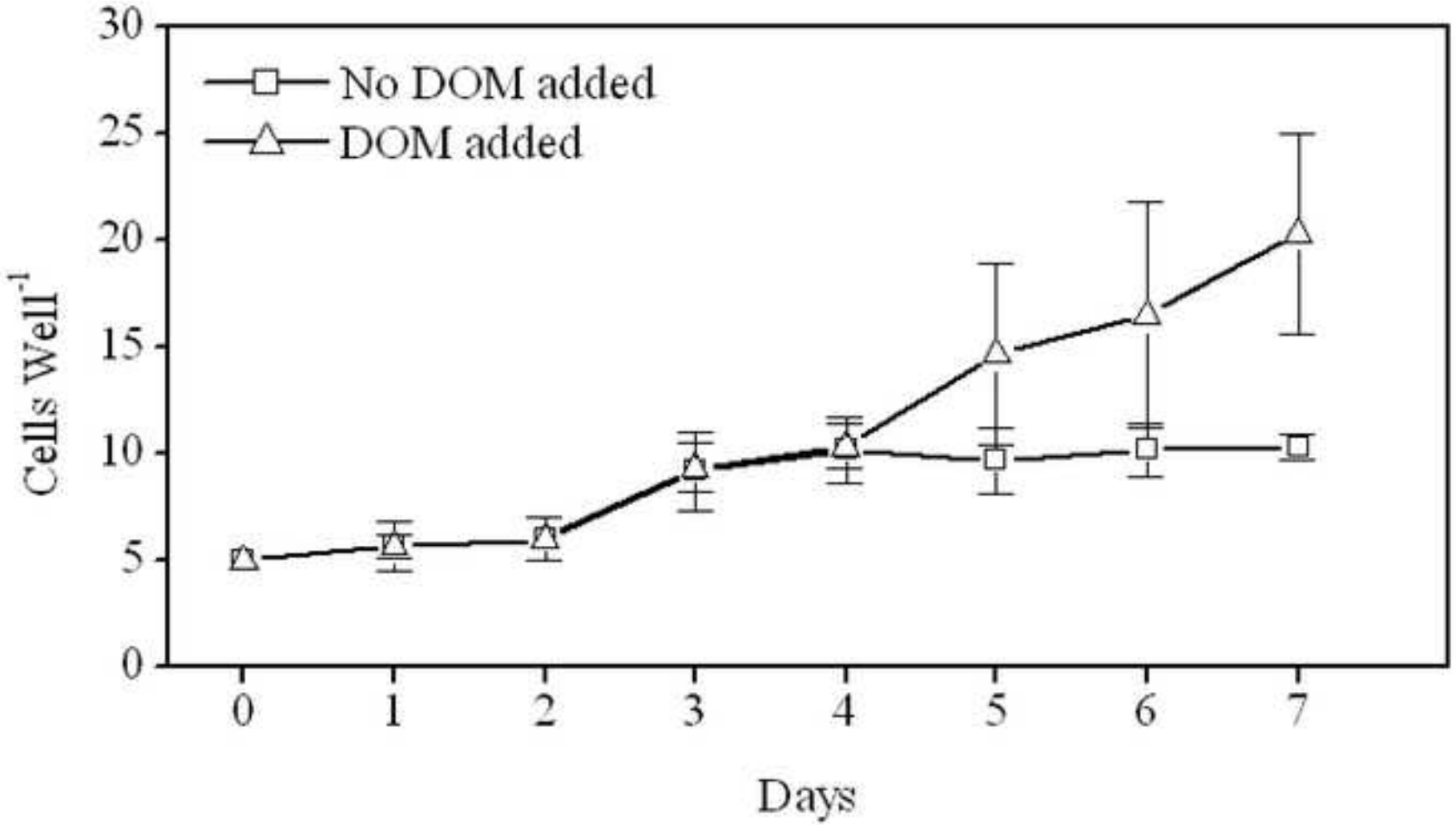

Figure 11

Click here to download high resolution image

Click here to view linked References

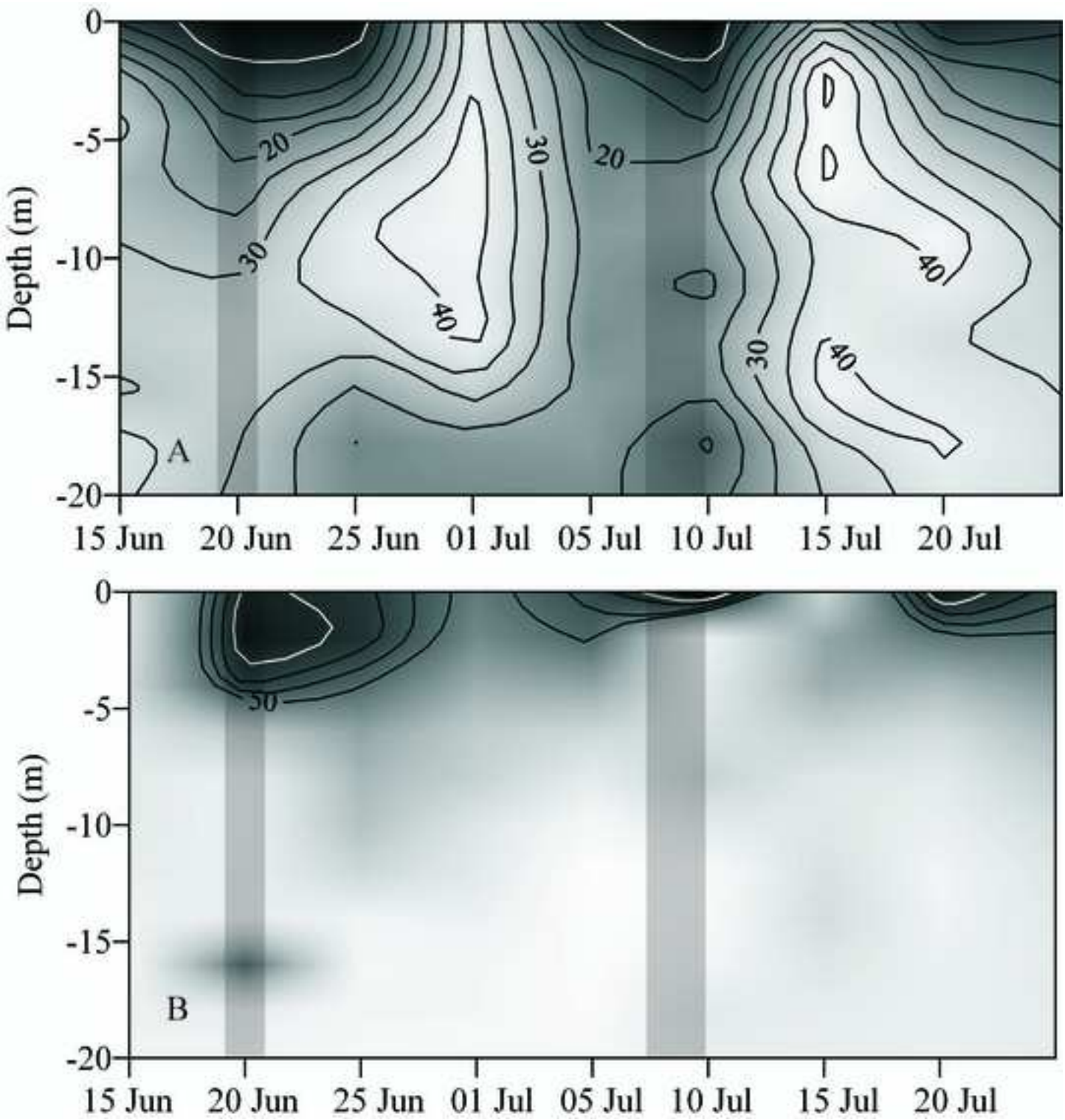

Figure 12

Click here to download high resolution image

Click here to view linked References